Syntheses and Physical Properties of Quasi-One-Dimensional Halogen-Bridged $Cu^{II}-Pt^{IV}$ Mixed-Metal Complexes $[Cu(chxn)_2][PtX_2(chxn)_2]X_4$

Takuya Kawashima,[†] Kenzi Takai,[†] Hidemitsu Aso,[‡] Toshio Manabe,[‡] Kouichi Takizawa,[‡] Chihiro Kachi-Terajima,[‡] Tomohiko Ishii,[‡] Hitoshi Miyasaka,[‡] Hiroyuki Matsuzaka,[‡] Masahiro Yamashita,*[,‡] Hiroshi Okamoto,[§] Hiroshi Kitagawa,[∥] Motoo Shiro,[⊥] and Koshiro Toriumi[#]

Graduate School of Human Informatics, Nagoya University, Chikusa-ku, Nagoya 464-8601, Japan, Graduate School of Science & PRESTO (JST), Tokyo Metropolitan University, Hachioji, Tokyo 192-0397, Japan, Graduate School of Frontier Science & PRESTO (JST), The University of Tokyo, Hongo, Bunkyo-ku, Tokyo 113-8656, Japan, Department of Chemistry, University of Tsukuba, Tsukuba 305-8571, Japan, and Rigaku Co., Akishima, Tokyo 196-8666, Japan, and Faculty of Science, Himeji Institute of Technology, Hyogo 678-1297, Japan

Received March 27, 2001

Quasi-one-dimensional halogen-bridged $Cu^{II}-Pt^{IV}$ mixed-metal complexes of the form $[Cu(chxn)_2][PtX_2(chxn)_2]X_4$, where chxn = 1*R*,2*R*-diaminocyclohexane and X is either Cl or Br, have been synthesized. The crystal structures of these compounds have been determined by single-crystal X-ray diffraction. The Cl-bridged compound crystallizes in the space group *I*222 with dimensions $a = 24.237(1)$ Å, $b = 5.103(1)$ Å, $c = 6.854(1)$ Å, and $V = 847.7(1)$ Å^3 and with $Z = 1$. The Br-bridged complex crystallizes in the space group *I*222 with dimensions $a = 23.700(8)$ Å, $b = 5.344(5)$ Å, $c = 6.978(8)$ Å, and $V = 883.8(8)$ Å^3 and with $Z = 1$. These structures are isomorphic to each other and to homometal $[Pt(chxn)_2][PtX_2(chxn)_2]X_4$ complexes. In these complexes, the planar $[Cu(chxn)_2]$ and the octahedral $[PtX_2(chxn)_2]$ groups are stacked alternatively with the axial bridging halogen ions, forming linear chain structures. The neighboring $[Cu(chxn)_2]$ and $[PtX_2(chxn)_2]$ moieties along the chains are linked by hydrogen bonds between amino hydrogens and the counteranions (X). Moreover, there are hydrogen bonds among the neighboring chains that form a two-dimensional hydrogen-bonded network parallel to the *bc* plane. Therefore, the Cu^{II} and Pt^{IV} units are two-dimensionally ordered. The *b* axes correspond to the $Cu^{II}-Pt^{IV}$ separations, which are shorter than those of $[Pt(chxn)_2][PtX_2(chxn)_2]X_4$ due to the smaller ionic radius of the Cu^{II} ions. In the XP spectra, the Pt^{IV} $4f_{7/2}$ and Pt^{IV} $4f_{5/2}$ binding energies in homometal $[Pt(chxn)_2][PtX_2(chxn)_2]X_4$ are lower than those of $[Cu(chxn)_2][PtX_2(chxn)_2]X_4$ (X = Cl and Br), indicating that the electron−phonon interaction in $Cu^{II}-Pt^{IV}$ compounds is stronger than that in $Pt^{II}-Pt^{IV}$ compounds. In the Raman spectra, $\nu(Pt^{IV}-X)$ of the homometal $Pt^{II}-Pt^{IV}$ complexes is lower than that of the $Cu^{II}-Pt^{IV}$ complexes, indicating again that the electron−phonon interaction in $Cu^{II}-Pt^{IV}$ compounds is stronger than that of $Pt^{II}-Pt^{IV}$ compounds. The temperature-dependent magnetic susceptibilities of the $Cu^{II}-Pt^{IV}$ complexes show weak antiferromagnetic interactions between Cu^{II} components along the chain axes.

Introduction

Recently low-dimensional compounds have attracted considerable attention due to their novel physical properties such as the Peierls transition, spin-Peierls transition, neutral−ionic transition, charge density wave (CDW) states, spin density wave (SDW) states, and superconductivity, etc.[1] Among these compounds, the quasi-one-dimensional halogen-bridged mixed-valence compounds (hereafter abbreviated as MX chains) have been extensively investigated during the last 20 years, since they exhibit a wide range of interesting physical properties. These include intense and dichroic intervalence charge-transfer bands, progressive resonance Raman spectra, luminescence with large Stokes shifts, midgap absorption attributable to solitons and polarons, large third-order nonlinear optical properties, one-dimensional model compounds of high-T_c copper oxide superconductors, etc.[2] The excited states and the relaxation process of these compounds have been investigated as a prototype material for one-dimensional electronic systems using pico- and femtosecond time-resolved optical methods.[3] The creation of solitons and polarons has been controlled by using the differences in the dimensionalities of the CDW states.[4] The third-

[†] Nagoya University.
[‡] Tokyo Metropolitan University.
[§] The University of Tokyo.
[∥] University of Tsukuba.
[⊥] Rigaku Co.
[#] Himeji Institute of Technology.

(1) *Extended Linear Chain Compounds*; Miller, J. S., Ed.; Plenum: New York, 1982; Vols. I−III.

(2) (a)Yamashita, M. In *New Functional Materials, Vol. C: Synthetic Process and Control of Functional Materials*; Tsuruta, T., Donoyama, M., Seno, M., Eds.; Elsevier Science Publisher: Tokyo, 1993; p 539. (b) Bishop, A. R.; Swanson, B. I. *Los Alamos Sci*. **1993**, *21*, 133. (c) Clark, R. J. H. *Adv. Infrared Raman Spectrosc*. **1983**, *11*, 133. (d) Okamoto, H.; Yamashita, M. *Bull. Chem. Soc. Jpn*. **1998**, *71*, 2023. (e) Yamashita, M.; Manabe, T.; Kawashima, T.; Okamoto, H.; Kitagawa, H. *Coord. Chem. Rev*. **1999**, *190−192*, 309.

(3) (a) Wada, Y.; Era, K.; Yamashita, M. *Solid State Commun*. **1988**, *67*, 953. (b) Ooi, H.; Kobayashi, T.; Yamashita, M. *Solid Sate Commun*. **1993**, *86*, 789. (c) Ooi, H.; Kobayashi, T.; Yamashita, M. *Chem. Phys. Lett*. **1993**, *210*, 384.

10.1021/ic010341t CCC: $20.00
Published on Web 11/14/2001

order nonlinear optical susceptibilities of these compounds are observed to be larger than that of poly(diacetylene).[5] Indeed recently a gigantic third-order nonlinear susceptibility has been observed in $[Ni(chxn)_2Br]Br_2$ (10^{-4} esu).[6]

From a theoretical viewpoint, the MX-chain compounds are considered as a Peierls−Hubbard system. In such as system the electron−phonon interaction (*S*), the electron-transfer energy (*T*), and the on-site and intersite Coulomb interactions (*U* and *V*, respectively) compete and/or cooperate with one another.[7] Originally, these MX chains were considered as a one-dimensional metallic state with half-filled d_{z^2} orbitals of the metals and filled p_z orbitals of the bridging halogens. However, it is well-known in these compounds that the one-dimensional metallic state is unstable and that the system is subsequently transferred to the insulating state via the electron−phonon interaction (*S*) and the electron correlation (*U*). In most MX chains, due to the strong electron−phonon interaction, the bridging halogens are distorted from the midpoints between the neighboring two metal atoms, giving rise to CDW states, or $M^{II}-M^{IV}$ mixed-valence states ($\cdots M^{II}\cdots X-M^{IV}-X\cdots M^{II}\cdots$). Accordingly, the half-filled metallic band is split into an occupied valence band and an unoccupied conduction band with a finite Peierls gap. Therefore, these compounds belong to the class II type of the Robin−Day classification for mixed-valence complexes.[8] The compounds are formulated as $[M^{II}(AA)_2][M^{IV}X_2(AA)_2]Y_4$ ($M^{II}-M^{IV}$ = $Pt^{II}-Pt^{IV}$, $Ni^{II}-Pt^{IV}$, $Pd^{II}-Pt^{IV}$, $Pd^{II}-Pd^{IV}$; X = Cl, Br, I, and mixed-halides; AA = ethylenediamine (en), 1*R*,2*R*-diaminocyclohexane (chxn), etc.; Y = ClO_4, BF_4, X, etc.). These MX chain compounds have two characteristic features when compared with inorganic semiconductors and organic conjugated polymers as follows: The magnitudes of the band gaps or CDW strengths can be tuned by varying chemical factors such as M, AA, X, and Y; in other words, the physical parameters (*S*, *T*, *U*, and *V*) can be tuned by substitution of various chemical factors. Moreover, the interchain interaction can be controlled via the intra- and interchain hydrogen-bond network between amino hydrogens and counteranions.

Theoretically it has been proposed that the M^{III} state or SDW state, where the bridging halogens are located at the midpoints between neighboring two metal ions ($-X-M^{III}-X-M^{III}-X-$), can be considered to be the more stable when there is a stronger on-site Coulomb interaction (*U*) compared to the electron−phonon interaction (*S*). Our group has been successful in synthesizing such compounds, formulated as $[Ni^{III}(chxn)_2X]Y_2$ (X = Cl, Br, or mixed-halides; Y = Cl, Br, mixed-halides, ClO_4, BF_4, or NO_3). The choice of Ni is because the Ni ion has a greater *U* compared with that of a Pd or Pt ion.[9] These Ni^{III} compounds show a very strong antiferromagnetic interaction among spins located on $3d_{z^2}$ orbitals at each Ni^{III} ion throughout the bridging halogens. These compounds belong to the class III type of the Robin−Day classification for mixed-valence complexes. The XP spectra, Auger spectra, and single-crystal reflectance spectra reveal that these Ni compounds are not Mott insulators but charge-transfer insulators, where the energy levels of the bridging halogens are located between the upper and lower Hubbard bands. Therefore, the electronic structures of the Ni compounds are similar to those of the starting materials of the copper oxide superconductors, except with respect to their dimensionality.

To summarize, for MX complexes with a stronger electron−phonon interaction (*S*), the oxidation states approach the $M^{II-}M^{IV}$ states. On the other hand, in the case of a stronger on-site Coulomb interaction (*U*), the oxidation states approach that of the M^{III} states.

More recently, we have succeeded in synthesizing single crystals of Ni−Pd mixed-metal compounds of the form $Ni_xPd_{1-x}(chxn)_2Br_3$, where the electron−phonon interaction (*S*) on $Pd^{II}-Pd^{IV}$ sites (CDW) and the on-site Coulomb interaction (*U*) on Ni^{III} sites (SDW) compete with one another. As a result, the $Pd^{II}-Pd^{IV}$ states are gradually changed to Pd^{III} states with an increasing Ni component, due to the greater *U* of the Ni sites (∼5 eV) compared with the *S* of the Pd sites (∼1 eV).[10]

Although at present most MX chain compounds have been composed of Pt, Pd, and Ni metal ions, one exception to this exists with $[Cu(en)_2][PtCl_2(en)_2](ClO_4)_4$.[11] In this Cu complex, interactions between the unpaired electrons on Cu^{II} and CT excitons and magnetic interactions between unpaired electrons on the Cu^{II} ions through the Pt^{IV} ions are anticipated. However, since the $[Cu(en)_2][PtCl_2(en)_2](ClO_4)_4$ is a one-dimensional structure, where each chain is separated with en and ClO_4 ions, $Pt^{II}-Pt^{IV}$ species as impurities may become easily substituted into this system during the sythesization process. Therefore, the formula is more accurately presented as $[Cu_{1-x}Pt_x(en)_2][PtCl_2(en)_2](ClO_4)_4$. The physical properties of this compound are considered to be mainly due to the presence of $Pt^{II}-Pt^{IV}$ species as contaminants in $[Cu_{1-x}Pt_x(en)_2][PtCl_2(en)_2](ClO_4)_4$. The pure $Cu^{II}-Pt^{IV}$ compound is considered to be difficult to obtain in the one-dimensional system. Previously, we have reported two-dimensional CDW systems formulated as $[M(chxn)_2][MX_2(chxn)_2]X_4$, where intra- and interchain two-dimensional hydrogen-bond networks are constructed between amino hydrogens and counteranions. Therefore, the M^{II} and M^{IV} units are distinguishable two-dimensionally. If this system is employed for $Cu^{II}-Pt^{IV}$ compounds, contamination of the $Pt^{II}-Pt^{IV}$ species can be effectively suppressed. According to such a strategy, we have tried to synthesize pure $[Cu(chxn)_2][PtX_2(chxn)_2]X_4$ (X = Cl and Br). In this paper, we will describe the syntheses and physical properties of $[Cu(chxn)_2][PtX_2(chxn)_2]X_4$ (X = Cl or Br).

Experimental Section

General Procedures and Chemicals. All syntheses were performed in air. All chemical reagents ($CuCl_2$, $CuBr_2$, methanol, chxn (=1*R*,2*R*-

(4) (a) Okamoto, H.; Toriumi, K.; Mitani, T.; Yamashita, M. *Phys. Rev. Lett*. **1992**, *69*, 2248. (b) Okamoto, H.; Kaga, Y.; Shimada, Y.; Oka, Y.; Iwasa, Y.; Mitani, T.; Yamashita, M. *Phys. Rev. Lett*. **1998**, *80*, 861.

(5) (a) Wada, Y.; Yamashita, M. *Jpn. J. Appl. Phys*. **1990**, *29*, 2744. (b) Iwasa, Y.; Funatsu, E.; Koda, T.; Yamashita, M. *Appl. Phys. Lett*. **1991**, *59*, 2219. (c) Iwasa, Y.; Funatsu, E.; Koda, T.; Yamashita, M. *Mol. Cryst. Liq. Cryst*. **1992**, *217*, 37.

(6) Kishida, H.; Matsuzaki, H.; Okamoto, H.; Manabe, T.; Yamashita, M.; Taguchi, Y.; Tokura, Y. *Nature* **2000**, *405*, 929.

(7) (a) Nasu. K. *J. Phys. Soc. Jpn*. **1983**, *52*, 3865. (b) Nasu. K. *J. Phys. Soc. Jpn*. **1983**, *53*, 302. (c) Nasu. K. *J. Phys. Soc. Jpn*. **1983**, *53*, 427. (d) Gammel, J. T.; Saxena, A.; Batstic, I.; Bishop, A. R.; Phillpot, S. R. *Phys. Rev. B* **1992**, *45*, 6408

(8) Robin, M. B.; Day, P. *Adv. Inorg. Radiochem*. **1967**, *10*, 247

(9) (a) Toriumi, K.; Wada, Y.; Mitani, T.; Bandow, S.; Yamashita, M.; Fujii. *J. Am. Chem. Soc*. **1989**, *111*, 2341. (b) Okamoto, H.; Toriumi, K.; Mitani, T.; Yamashita, M. *Phys. Rev B* **1990**, *42*, 10381. (c)Yamashita, M.; Manabe, T.; Inoue, K.; Kawashima, T.; Okamoto, H.; Kitagawa, H.; Mitani, T.; Toriumi, K.; Miyamae, H.; Ikeda, R. *Inorg. Chem*. **1999**, *38*, 1894

(10) (a) Yamashita, M.; Ishii, T.; Matsuzaka, H. Manabe, T.; Kawashima. T.; Okamoto, H.; Kitagawa, H.; Mitani, T.; Marumoto, K.; Kuroda, S. *Inorg. Chem.* **1999**, *38*, 5124. (b) Manabe, T.; Kawashima, T.; Yamashita, M.; Okamoto, H.; Kitagawa, H.; Mitani, T.; Inokuchi, M.; Yakushi, K. *Synth. Met.* **1997**, *86*, 2233. (c) Marumoto, K.; Kuroda, S.; Manabe, T.; Yamashita, M. *Phys. Rev. B* **1999**, *60*, 7699. (d) Wakabayashi, Y.; Wakabayashi, N.; Yamashita, M.; Manabe, T.; Matsushita, N. *J. Phys. Soc. Jpn*. **1999**, *68*, 3948.

(11) Oshio, H.; Toriumi, K.; Bandow, S.; Miyagawa, K.; Kurita, S. *J. Chem. Soc., Dalton Trans*. **1990**, 1013.

Table 1. Crystal Data

emp formula	$C_{24}H_{56}N_8PtCuCl_6$	$C_{24}H_{56}N_8PtCuBr_6$
fw	928.1	1194.8
cryst size (mm^3)	0.33 × 0.10 × 0.06	0.20 × 0.20 × 0.08
a/Å	24.237(1)	23.700(8)
b/Å	5.103(1)	5.344(5)
c/Å	6.854(1)	6.978(4)
V/$Å^3$	847.7(1)	883.8(8)
Z	1	1
space group	*I*222	*I*222
D_{calcd} (g/cm^3)	1.816	2.245
no. of observns	1243	571
λ/Å	0.710 69	0.710 70
temp (K)	296	123
residuals: R;[a] R_w[b]	0.019, 0.024	0.037, 0.098

[a] $R = \sum||F_o| - |F_c||/\sum|F_o|$. [b] $R_w = [\sum w(F_o - F_c)^2/\sum wF_o^2]^{1/2}$.

diaminocyclohexane), $K_2[PtCl_4]$, $PtBr_2$, 30% H_2O_2, 37% HCl, 49% HBr, LiCl, and LiBr) were purchased form Wako Pure Chemical Industry, Ltd. All chemicals used were reagent grade.

Preparation of $[Cu(chxn)_2]X_2$ (X = Cl and Br). CuX_2 (0.01 mol; X = Cl or Br) was dissolved into methanol (50 mL), into which the chxn ligand (0.025 mol) was subsequently added. The methanol solution was evaporated until precipitates were formed. $[Cu(chxn)_2]X_2$ was recrystalized from the hot methanol solution (yield = ca. 80%).

Preparation of $[PtX_2(chxn)_2]X_2$ (X = Cl and Br). The starting material, $[Pt(chxn)_2]X_2$, was obtained by a method previously described.[9b] $[PtX_2(chxn)_2]X_2$ was obtained via an oxidation reaction of $[Pt(chxn)_2]X_2$ (0.01 mol) using H_2O_2 (10 mL) and HX (10 mL) in an aqueous solution (50 mL) and subsequently recrystallized from an aqueous solution (yield = ca. 85%).

Preparation of $[Cu(chxn)_2][PtX_2(chxn)_2]X_4$ (X = Cl or Br). Equimolar amounts of $[Cu(chxn)_2]X_2$ (0.005 mol) and $[PtX_2(chxn)_2]X_2$ (0.005 mol) were dissolved in water (25 mL). Excess amounts of LiX (0.05 mol; X = Cl or Br) were added to these solutions. After a few days, crystals were formed. Elemental analysis of Cu and Pt were carried out using the ICP method. Typical analyses were as follows.

Calcd for $C_{24}H_{56}N_8Cl_6CuPt$: Pt, 21.03; Cu, 6.85; C, 31.06; H, 6.08; N, 12.07. Found: Pt, 20.64; Cu, 6.81; C, 30.98; H, 5.84; N, 12.13.

Calcd for $C_{24}H_{56}N_8Br_6CuPt$: Pt, 16.33; Cu, 5.32; C, 24.13; H, 9.38; N, 4.72. Found: Pt, 16.41; Cu, 5.69; C, 24.13; H, 9.35; N, 4.65.

Single-crystal X-ray structural measurements were carried out. The diffracted intensity data was collected on a RIGAKU AFC-5 four-circular instrument for $[Cu(chxn)_2][PtCl_2(chxn)_2]Cl_4$ at room temperature and on a Rigaku RAXIS-IV imaging plate area detector for $[Cu(chxn)_2][PtBr_2(chxn)_2]Br_4$ at 123 K, both using graphite-monochromated Mo Kα radiation. The crystal data are listed in Table 1. The structures were resolved using heavy atom methods and refined using full-matrix least-squares techniques.

The measurements of XP spectra were performed using an Escalab MKII (VG Scientific) photoelectron spectrometer with Mg Kα as the excitation light source. For these measurements all the samples were ground into powder form in an N_2-gas-filled glovebox attached to the preparation chamber. This allows the powdered samples to be inserted into the high-vacuum chamber without subsequent exposure to air. The base pressure of the analysis chamber was in the 10^{-10} Torr range.

IR spectra were measured in the temperature range of 11−300 K using a Nicolet FTIR 800 spectrometer with a Daikin CryoKelvin cryostat that has KRS-5 optical windows. IR detectors of TGS and MCT were used.

Raman spectra were measured using 514.5 nm Ar^+ excitation (Spectra-Physics model 2017 Ar^+ laser) with a JASCO NR-1800 laser Raman spectrometer. Detection of the scattered radiation was made using a cooled photometrics CC 200 CCD camera system with an operating temperature of 153 K. The laser power at the crystals was kept at less than 1 mW to avoid damage to samples. The wavenumber calibration was effected by reference to the Raman spectrum of Indene or to the emission spectrum of a Ne lamp.

For the measurements of the polarized reflectance spectra, a halogen−tungsten incandescent lamp was used. Light from the lamp was used by a concave mirror on the entrance slit of a 25 cm grating monochromator (Jasco CD 25). The monochromatic light from the exit slit was passed through a polarizer and was focused on the specific surface of a single-crystal sample by using an optical microscope. Reflected light from the sample was focused by a concave mirror on the detector (a PdS cell or a photomultiplier tube).

The magnetic susceptibilities of polycrystalline samples were measured on a Quantum Design SQUID magnetometer in an applied magnetic field of 2000 G from 2 to 300 K.

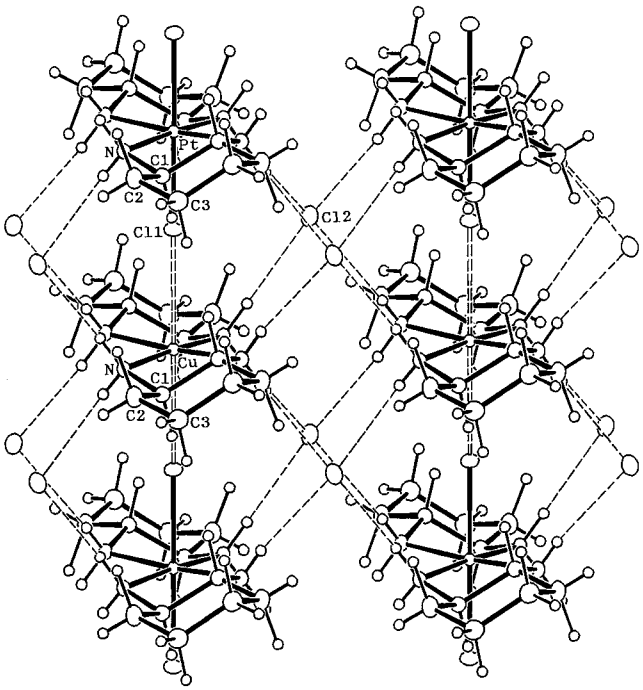

Figure 1. Crystal structure of $[Cu(chxn)_2][PtCl_2(chxn)_2]Cl_4$ with atomic numbers. The thermal ellipsoids are shown at the 30% probability level.

Results and Discussion

A precise knowledge of the ratios of Cu and Pt ions in these synthesized compounds is an important prerequisite for understanding their properties. The ICP elemental analytical method was applied to the compounds, and a ratio of Cu and Pt of 1:1 was obtained. Therefore, the chemical formula is accurately described as $[Cu(chxn)_2][PtX_2(chxn)_2]X_4$ (X = Cl or Br). This analysis is confirmed using single-crystal X-ray diffraction, as described below.

The crystal structures of $[Cu(chxn)_2][PtX_2(chxn)_2]X_4$ (X = Cl or Br) are isomorphous to each other and also to those of homometal $[Pt(chxn)_2][PtX_2(chxn)_2]X_4$ (X = Cl or Br) compounds although their metal ions are different from each other. The crystal structure of X = Cl is shown in Figure 1. The relevant bond lengths of these compounds are listed in Table 2, along with those of the corresponding $Pt^{II}-Pt^{IV}$ mixed-valence compounds. The ratios between Cu^{II} and Pt^{IV} moieties are 1:1 for both compounds, as observed in the ICP elemental analyses. The square-planar $[Cu(chxn)_2]$ and the hexacoordinated octahedral $[PtCl_2(chxn)_2]$ are stacked alternatively with the axial bridging halogens, forming linear chain structures. The neighboring $[Cu(chxn)_2]$ and $[PtCl_2(chxn)_2]$ moieties along the chains are linked by hydrogen bonds between amino hydrogens and counter Cl ions. Moreover, there are the hydrogen bonds among the neighboring chains, which produce two-dimensional hydrogen-bonded networks parallel to the *bc* plane as shown in Figure 1. Therefore, the Cu and Pt units are two-dimensionally ordered and are distinguishable between one another. The Cu−Pt bond

Table 2. Relevant Bond Lengths (Å)

	$M^{II}\cdots X$	$M^{IV}-X$	M−N	$M^{II}-Pt^{IV}$	ρ
$[Cu(chxn)_2][PtCl_2(chxn)_2]Cl_4$	2.804(1)	2.299(1)	2.040(2)	5.103(1)	0.8199
$[Pt(chxn)_2][PtCl_2(chxn)_2]Cl_4$	2.834(2)	2.324(2)	2.056(4)	5.158(1)	0.8200
$[Cu(chxn)_2][PtBr_2(chxn)_2]Br_4$	2.899(2)	2.445(2)	2.049(5)	5.344(5)	0.8460
$[Pt(chxn)_2]$ $[PtBr_2(chxn)_2]Br_4$	2.882(5)	2.497(5)	2.098(7)	5.379(1)	0.8664

Table 3. Binding Energies (eV)

	Pt^{IV}	
compd	$4f_{7/2}$	$4f_{5/2}$
$[PtCl_2(chxn)_2]Cl_2$	75.2	78.4
$[Cu(chxn)_2][PtCl_2(chxn)_2]Cl_4$	75.2	77.4
$[Pt(chxn)_2][PtCl_2(chxn)_2]Cl_4$	74.4	77.4
$[PtBr_2(chxn)_2]Br_2$	75.1	78.3
$[Cu(chxn)_2]$ $[PtBr_2(chxn)_2]Br_4$	75.1	78.2
$[Pt(chxn)_2][PtBr_2(chxn)_2]Br_4$	73.8	77.6

is aligned along the *b* axis, which in the case of the Cl-bridged compound is shorter than that in the Br-bridged compound, due to the smaller ionic radius of Cl ions. The *b* axes of the $[Cu(chxn)_2][PtX_2(chxn)_2]X_4$ are shorter than those of $[Pt(chxn)_2][PtX_2(chxn)_2]X_4$ due to the smaller Cu ionic radius. The $Cu^{II}\cdots X$ and $Pt^{IV}-X$ distances in the $Cu^{II}-Pt^{IV}$ compounds are shorter than the $Pt^{II}\cdots X$ and $Pt^{IV}-X$ distances in the $Pt^{II}-Pt^{IV}$ mixed-valence compounds, respectively, due to the smaller ionic radius. The distortion ratios of the bridging halogens, defined as $\rho = M^{IV}-X/M^{II}\cdots X$, are important for evaluating their oxidation states. The $\rho = 1$ indicates that the oxidation states of metal ions are +3, which is observed in $[Ni^{III}(chxn)_2X]X_2$. When the ρ is approaching 1, the oxidation states are approaching +3. The ρ values of the Cl-bridged complexes are smaller than those of the Br-bridged complexes. The ρ value of the Cl-bridged $Cu^{II}-Pt^{IV}$ complex is a little smaller than that of the Cl-bridged $Pt^{II}-Pt^{IV}$ complex. The ρ value of the Br-bridged $Cu^{II}-Pt^{IV}$ complex is much smaller than that of the Br-bridged $Pt^{II}-Pt^{IV}$ complex. Such results indicate that the electron−phonon interactions of the Cl-bridged complexes are stronger than those of the Br-bridged complexes, and the electron−phonon interactions of the $Cu^{II}-Pt^{IV}$ complexes are stronger than those of the $Pt^{II}-Pt^{IV}$ complexes. The *c* axes in $Cu^{II}-Pt^{IV}$ compounds, which are in the direction of the interchain hydrogen bonds, are longer than those of the $Pt^{II}-Pt^{IV}$ mixed-valence compounds. Such a negative correlation between the *b* and *c* axes is also observed in $M(chxn)_2XY_2$ (M = Ni, Pd and Pt; X = Cl or Br; Y = X and ClO4).[9c] The $Cu^{II}-N$ distances in the $Cu^{II}-Pt^{IV}$ compounds are shorter than the $Pt^{II}-N$ distances in the $Pt^{II}-Pt^{IV}$ compounds.

X-ray photoelectron spectroscopy (XPS) is a good probe for evaluating the oxidation states in the mixed-valence compounds. Previously we have measured the XPS of $[M(en)_2][MX_2(en)_2](ClO_4)_4$.[12] In the order from Cl to I, the binding energies of Pt^{II} 4f increase, while the binding energies of Pt^{IV} 4f decrease, indicating that the oxidation states of the Pt units approach those of Pt^{III} as we move from Cl- to I-bridged compounds. The binding energies of Pt^{IV} 4f in $[Pt(chxn)_2][PtX_2(chxn)_2]X_4$ are lower than those in $[Cu(chxn)_2][PtX_2(chxn)_2]X_4$ and of the starting material $[PtX_2(chxn)_2]X_2$, indicating that the oxidation states of the $Pt^{II}-Pt^{IV}$ compounds more closely approach those of Pt^{III} when compared with those of $Cu^{II}-Pt^{IV}$ compounds (Table 3). This is due to a stronger electron−phonon interaction in $Cu^{II}-Pt^{IV}$ compounds. A similar phenomena is also observed in the heterometal compounds of the form $[M(en)_2][PtX_2(en)_2](ClO_4)_4$ (M = Ni and Pd).[12]

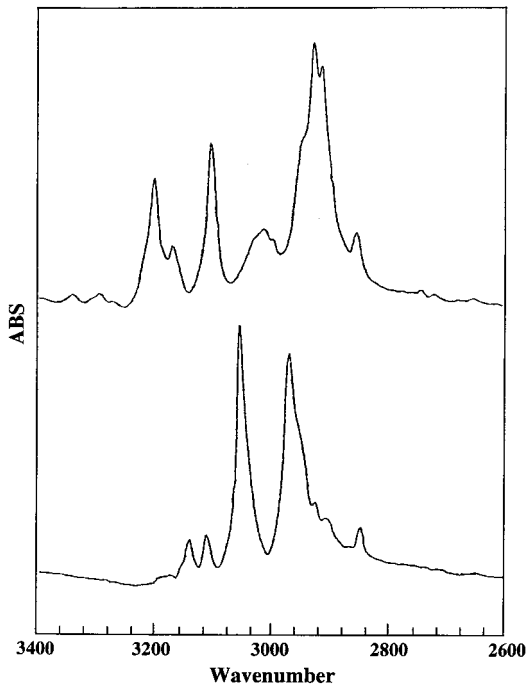

Figure 2. IR spectra of ν(N−H) in $[Cu(chxn)_2][PtCl_2(chxn)_2]Cl_4$ (top) and $[Pt(chxn)_2][PtCl_2(chxn)_2]Cl_4$ (bottom).

The IR spectra of ν(N−H) in the two-dimensional hydrogen-bond network provide another good probe for evaluating the oxidation states.[13] The magnitude of the splitting of ν(N−H) is influenced by the oxidation states of the compounds. In the IR spectra of $M(chxn)_2Br_3$, the Ni compound shows a singlet ν(N−H), due to the +3 oxidation state, while a doublet ν(N−H) is observed in the Pt and Pd compounds due to the presence of oxidation states of +2 and +4. Moreover, the splitting of the Pd compound is smaller than that of the Pt compound due to the smaller electron−phonon interaction. The IR spectra of $[M(chxn)_2][PtX_2(chxn)_2]X_4$ (X = Pt and Cu) are composed of two ν(N−H) (Figure 2). The magnitudes of the splitting of $Cu^{II}-Pt^{IV}$ compounds is larger than that of $Pt^{II}-Pt^{IV}$ compounds, indicating that the electron−phonon interaction in $Cu^{II}-Pt^{IV}$ compounds is stronger than that in $Pt^{II}-Pt^{IV}$ compounds. These results are consistent with the crystal structural and XPS data described above.

In the single-crystal reflectance spectra of the $Cu^{II}-Pt^{IV}$ complexes, the intense CT bands are observed in the visible region along the chain axes. The CT band edge of the Cl-bridged $Cu^{II}-Pt^{IV}$ is higher than that of the Br-bridged complex, indicating the electron−phonon interaction of the Cl-bridged complex is stronger than that of the Br-bridged complex. Such a result is consistent with those of the crystal structures.

As a final confirmation of oxidation states we have measured the resonant Raman spectra of these compounds. In the $M^{II}-M^{IV}$ mixed-valence compounds, an overtone progression of

(12) (a) Yamashita, M.; Matsumoto, N.; Kida, S. *Inorg Chim. Acta* **1978**, *31*, L381. (b) Yamashita, M.; Murase, I.; Ikemoto, I.; Ito, T. *Bull. Chem. Soc. Jpn.* **1985**, *58*, 2697. (c)Yamashita, M.; Murase, I.; Ito, T.; Wada, Y.; Mitani, T.; Ikemoto, I. *Bull. Chem. Soc. Jpn*. **1985**, *58*, 1336.

(13) Okaniwa, K.; Okamoto, H.; Mitani, T.; Toriumi, K.; Yamashita, M. *J. Phys. Soc. Jpn*. **1991**, *60*, 997.

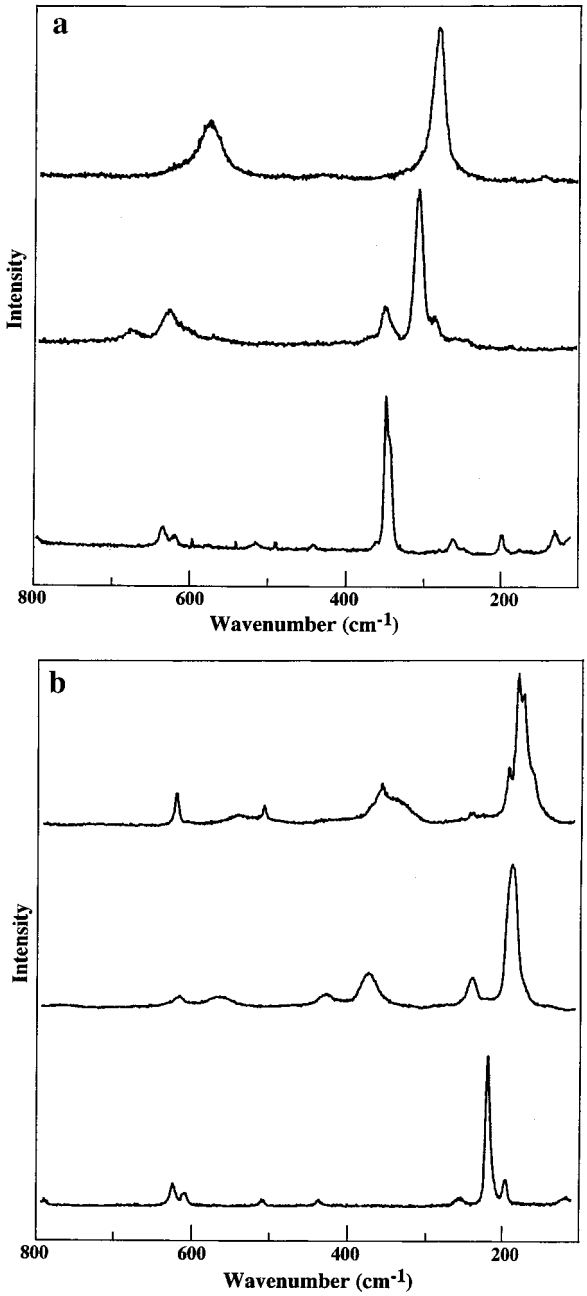

Figure 3. (a) Raman spectra of $[Pt(chxn)_2][PtCl_2(chxn)_2]Cl_4$ (top), $[Cu(chxn)_2][PtCl_2(chxn)_2]Cl_4$ (middle), and $[PtCl_2(chxn)_2]Cl_2$ (bottom). (b) Raman spectra of $[Pt(chxn)_2][PtBr_2(chxn)_2]Br_4$ (top), $[Cu(chxn)_2][PtBr_2(chxn)_2]Br_4$ (middle), and $[PtBr_2(chxn)_2]Br_2$ (bottom).

$\nu(M^{IV}-X)$ is usually observed. The energies of $\nu(M^{IV}-X)$ correspond to their oxidation states; that is, as the oxidation state approaches +3, the energies decrease. $\nu(Pt^{IV}-X)$ in the $Pt^{II}-Pt^{IV}$ compounds are lower than those of the $Cu^{II}-Pt^{IV}$ compounds and of the starting materials $[PtX_2(chxn)_2]X_2$, indicating that the electron−phonon interaction in the $Cu^{II}-Pt^{IV}$ compounds is stronger than that of the $Pt^{II}-Pt^{IV}$ compounds (Figure 3). These results are consistent with those of the above XPS and IR spectra.

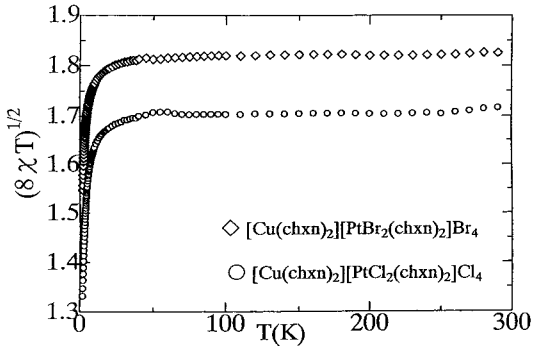

Figure 4. Temperature dependences of magnetic moments (μ_B) in $[Cu(chxn)_2][PtCl_2(chxn)_2]Cl_4$ and $[Cu(chxn)_2][PtBr_2(chxn)_2]Br_4$.

The temperature dependence of the magnetic susceptibilities was measured from 2 K to room temperature. The ESR spectra of these compounds show an axial pattern with the unpaired electron on the $d_{x^2-y^2}$ orbitals, perpendicular to the chain axes. Therefore, the magnetic susceptibilities show a very weak antiferromagnetic interaction at very low temperature (Figure 4). The antiferromagnetic interaction of the Cl-bridged compound is seemed to be stronger than that of the Br-bridged complex. This is due to the shorter $Cu^{II}\cdots Cu^{II}$ distance in the Cl-bridged complex compared with that of the Br-bridged complex.

Conclusion

We have been successful in synthesizing the pure $Cu^{II}-Pt^{IV}$ mixed-metal compounds $[Cu(chxn)_2][PtX_2(chxn)_2]X_4$ (X = Cl and Br) for the first time. This is due to introducing the two-dimensional hydrogen-bond networks into these compounds. Judging from the results of the crystal structures, IR, XPS, reflectance spectra, and Raman spectra, the electron−phonon interaction of the $Cu^{II}-Pt^{IV}$ mixed-metal complexes are stronger than those of the $Pt^{II}-Pt^{IV}$ mixed-valence complexes. This is due to the difference of the energy levels between 3d−5d in the $Cu^{II}-Pt^{IV}$ mixed-metal compounds and 5d−5d in the $Pt^{II}-Pt^{IV}$ mixed-valence compounds.

Acknowledgment. This work was partly supported by a Grant-in-Aid for Science Research on Priority Areas ("Metal-assembled Complexes") from the Ministry of Education, Science, and Culture of Japan.

Supporting Information Available: X-ray crystallographic data (CIF files) for $[Cu(chxn)_2][PtX_2(chxn)_2]X_4$, including tables of the atomic coordinations, bond angles, and bond lengths. This material is available free of charge via the Internet at http://pubs.acs.org.

IC010341T